PAPER

Quantifying temporal and spatial variations in sediment, nitrogen and phosphorus transport in stream inflows to a large eutrophic lake†

J. M. Abell,[*a] D. P. Hamilton[a] and J. C. Rutherford[b]

High-frequency sampling of two major stream inflows to a large eutrophic lake (Lake Rotorua, New Zealand) was conducted to measure inputs of total suspended sediment (TSS), and fractions of nitrogen and phosphorus (P). A total of 17 rain events were sampled, including three during which both streams were simultaneously monitored to quantify how concentration–discharge (Q) relationships varied between catchments during similar hydrological conditions. Dissolved inorganic nitrogen (DIN) concentrations declined slightly during events, reflecting dilution of groundwater inputs by rainfall, whereas dissolved inorganic P (PO_4–P) concentrations were variable and unrelated to Q, suggesting dynamic sorptive behaviour. Event loads of total nitrogen (TN) were predominantly DIN, which is available for immediate uptake by primary producers, whereas total phosphorus (TP) loads predominantly comprised particulate P (less labile). Positive correlations between Q and concentrations of TP (and to a lesser extent TN) reflected increased particulate nutrient concentrations at high flows. Consequently, load estimates based on hourly Q during storm events and concentrations of routine monthly samples (mostly base flow) under-estimated TN and TP loads by an average of 19% and 40% respectively. Hysteresis with Q was commonly observed and inclusion of hydrological variables that reflect Q history in regression models improved predictions of TN and TP concentrations. Lorenz curves describing the proportions of cumulative load *versus* cumulative time quantified temporal inequality in loading. In the two study streams, 50% of estimated two-year loads of TN, TP and TSS were transported in 202–207, 76–126 and 1–8 days respectively. This study quantifies how hydrological and landscape factors can interact to influence pollutant flux at the catchment scale and highlights the importance of including storm transfers in lake loading estimates.

Environmental impact

Quantifying nutrient and sediment inputs to lakes is essential for managing water quality yet the episodic nature of hydrological processes imposes variations to material fluxes that are inadequately resolved by routine monitoring programmes. The extensive high-frequency dataset collected during this study enabled variations in nitrogen, phosphorus and suspended sediment loading to a nationally iconic lake be examined in detail. Temporal (within catchment) and spatial (between catchment) differences in the relative importance of pollutant source areas were highlighted and shortcomings of common approaches to estimate external loads to lakes are quantified. By relating variations in loading to factors such as land use, geomorphology and antecedent hydrological conditions, this study furthers understanding of pollutant source–pathway–receptor interactions in lake catchments.

Introduction

Excess sediment and nutrient loading can have major adverse ecological impacts on receiving aquatic ecosystems.[1,2] Characterising spatial and temporal variations in fluxes of these potential pollutants through hydrological landscapes is therefore necessary to inform the implementation of actions (*e.g.* best agricultural management practices) designed to mitigate water pollution.[3] Additionally, resource managers require precise estimates of sediment and nutrient loads to receiving waters to monitor compliance with water quality standards, as well as to provide robust input data for water quality models that are increasingly used to help to understand ecosystem processes.[4,5]

Quantifying pollutant flux in surface streams requires knowledge of both discharge (Q) and determinand concentration, with the latter typically measured at lower frequency.

[a]*Environmental Research Institute, University of Waikato, Private Bag 3105, Hamilton 3240, New Zealand. E-mail: jma27@waikato.ac.nz; Fax: +64 7 838 4324; Tel: +64 7 858 5046*

[b]*National Institute of Water and Atmospheric Research, P.O. Box 11-115, Hamilton 3216, New Zealand*

† Electronic supplementary information (ESI) available. See DOI: 10.1039/c3em00083d

Although infrequent (*e.g.* monthly) measurements may suffice for reasonable estimation of sediment and nutrient loads during base flow conditions (but see Jordan *et al.*[6] for discussion of variable base flow loading), the potential for high temporal variation in determinand concentrations following rain events necessitates high-frequency sampling to accurately estimate loads conveyed in storm flow, particularly in low-order streams that respond quickly to rainfall.[7-9] In addition to informing load estimation, determinand concentration–Q relationships derived using high-frequency sampling can provide insight into the dominant sources and transport mechanisms of sediments and nutrients in catchments. This ability reflects the role of a catchment as a filter which mediates the downstream transport of pollutants, and, consequently, temporal variations in concentration during storm flows provide a signature that integrates the effects of complex upstream hydrological and biogeochemical interactions.[10-12]

Suspended sediment concentration typically increases in storm flow due to erosive processes, while nutrient concentrations may either increase or decrease due, for example, to flushing from critical source areas or dilution by rainwater respectively (*e.g.* ref. 13–15). In addition to Q, concentration may also vary in association with other hydrological variables that influence catchment transport processes such as soil moisture content.[16] Furthermore, when there is a relationship between concentration and Q, it may be non-monotonic, *i.e.* there may be hysteresis related to differences in concentration at particular Q depending on whether Q is increasing or receding.[17,18] The occurrence of a concentration peak before maximum Q (Q_{max}) during a hydrological event suggests a 'first flush' effect, attributed to mobilisation of sediments or nutrients accumulated in critical source areas on land or channel bed stores since a prior event (*e.g.* ref. 15), assuming that the flushing process is source- and not transport-limited.[19] Alternatively, the occurrence of a concentration peak during the recessing limb of the hydrograph has been interpreted to indicate slow diffuse delivery of pollutant to the channel (*e.g.* ref. 17). The potential for determinand concentrations to correlate positively with Q can contribute to temporal inequality in pollutant loading, *i.e.* a proportion of the cumulative load for a time period may be transported in a disproportionately short period of time. Such inequality can be quantified using Lorenz curves (Fig. 1). Lorenz curves are typically used to describe the cumulative distribution function of economic variables[20] but have recently been used to quantify temporal inequality in both Q and daily nutrient loads estimated from monthly measurements.[21]

The concentration–Q relationship may vary between catchments depending on individual characteristics such as land use. For example, Siwek *et al.*[22] found that nitrate (NO_3) concentration was positively correlated with Q in a woodland catchment (attributed to entrainment of NO_3 in soil by surface run off), whereas the relationship was negative in an agricultural catchment (attributed to dilution of polluted stream water by rainwater). Improving understanding of how landscape characteristics such as land use and hydrogeomorphology interact to influence sediment and nutrient transport has been identified as a research priority[5,23] and is important to aid
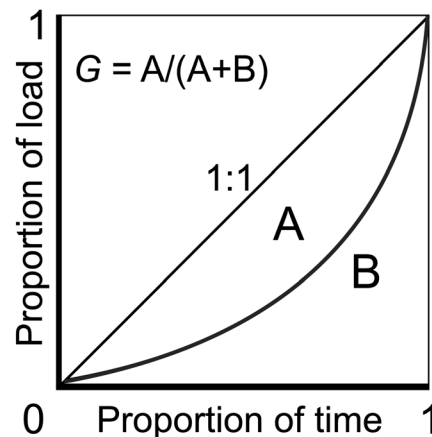

Fig. 1 Example of Lorenz curve used to examine the relationship between the proportion of a total load transported and the proportion of time elapsed during a defined period. The Gini coefficient (G) quantifies temporal inequality in loading from a scale of 0–1, where 0 implies that loading occurs at a constant rate and 1 implies that all loading occurs during the shortest time step.

development of models of pollutant transport in catchments, calibration of which is frequently constrained by lack of data relating to pollutant concentrations at high Q.[24] In the case of nutrients, there is specific need to consider variations related to individual fractions (*e.g.* dissolved and particulate) due to the differing bioavailability of various nitrogen and phosphorus forms and their subsequent discrepant potential to contribute to eutrophication in downstream waters.[25,26]

This study focuses on two stream inflows to a large eutrophic lake and examines temporal variations in suspended sediment, nitrogen and phosphorus loading during a range of Q. High frequency event-based sampling was conducted over an extended period (2+ years) which included concurrent sampling of both streams in order to investigate spatial variations in pollutant transport between the two catchments during similar hydrological conditions. The objectives were: (1) to quantify temporal (within-catchment) variations in suspended sediment and nutrient concentration in both base and storm flow; (2) to investigate how temporal changes in concentration–Q relationships can vary spatially (between sub-catchments upstream of a common lake ecosystem); and (3) to improve understanding of the potential for nutrients conveyed in storm flow to promote downstream eutrophication.

Methods

Study catchments

Event-based water sampling was undertaken of two stream inflows (Fig. 2) to Lake Rotorua, a large (81 km^2), eutrophic and polymictic lake in the Bay of Plenty Region of New Zealand. The local igneous geology is complex with a series of large aquifers that are distinct from surface water catchments.[27] Soils comprise deep, porous sands or loams that are high in allophane.[28] Water quality in Lake Rotorua has declined since at least the 1960s due to excess nutrient loading and, as a result, the lake is eutrophic, experiences undesirable
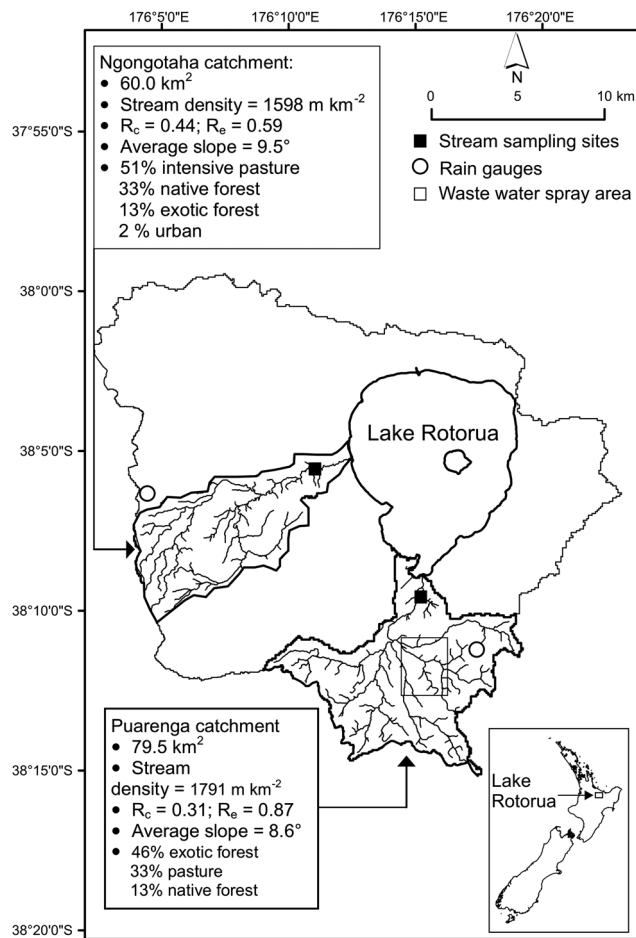
Fig. 2 Location of Lake Rotorua catchment, study stream surface catchments, monitoring locations and rain gauges. R_c, circularity ratio; R_e, elongation ratio.

algal blooms and is now a priority for remediation.[29,30] The lake has nine major stream inflows which supply approximately 66% of the total input of water.[31] Of these, the Ngongotaha and Puarenga streams have the two largest surface sub-catchments and the fourth and second greatest mean Q respectively.[31] Both streams are estimated to convey a high proportion of water in storm flow: 44% and 36% respectively.[32] Median discharge (Q_{50}) is similar in the two streams (Ngongotaha = 1.90 m^3 s^{-1}, Puarenga = 1.92 m^3 s^{-1}; May 2010–August 2012), although base flow is typically lower in the Ngongotaha Stream which has a more elongated catchment with lower drainage density than the Puarenga Stream catchment (Fig. 2). The Ngongotaha Stream catchment predominantly comprises pastoral agriculture with forested areas on steeper slopes. A sampling site was located upstream of the township of Ngongotaha. The dominant land use in the Puarenga Stream catchment is exotic coniferous forest comprising mostly *Pinus radiata*, although there is some pastoral agriculture (dry stock and dairy farms) and suburban land use immediately upstream of the sampling location (Fig. 2). The Rotorua Wastewater Treatment Plant is situated downstream of the Puarenga sampling location although treated sewage from the plant is discharged to land upstream

of the sampling location at the Rotorua Land Treatment System where effluent has been spray-irrigated over a 193 ha forested area since 1991.[33] The Whakarewarewa geothermal area is immediately upstream of the sampling location.

Sampling methods

The Ngongotaha Stream was sampled 2.5 km from the lake and Q was recorded at a permanent gauge sited 80 m further upstream. Precipitation (mm; hereafter 'rainfall') was measured at a permanent gauge sited at Upper Oturoa Road, 9 km to the north-west (Fig. 2). The Puarenga Stream was sampled 2.1 km from the lake and Q was recorded at a permanent gauge sited 800 m downstream. Rainfall was measured at a permanent gauge sited 3 km to the south-east (Whakarewarewa; Fig. 2). Discharge was measured every 15–60 minutes and rainfall every hour. Soil moisture was measured using an *in situ* dielectric probe situated at the rain gauge site north of Ngongotaha Stream catchment (Fig. 2).

Stream water at both sites was sampled at high frequency over 1–5 day periods coinciding with forecasted rainfall during different seasons between May 2010 and July 2012. The objective was to sample during pre-event base flow and throughout the rising and recessing limbs of the hydrograph. Stream water (0.5–1 L) was sampled from mid base flow water depth using automatic samplers (Manning VST portable) programmed to sample at 1–2 h frequency over the duration of each sampling period. A small number of supplementary samples were also collected manually from the same sites (<5% of samples). Sample bottles and hoses were acid-washed (10% HCl) and triple-rinsed with analytical grade deionised water (Millipore Co.) prior to deployment during each sampling period. Samplers were filled with ice and samples retrieved daily before the ice melted. Sub-samples for dissolved nutrient analysis were taken by filtration in the field (0.5 μm, Advantec GF GC-50) using acid-washed syringes during daily retrieval. Filtered and unfiltered sub-samples for nutrient analysis were stored in acid-washed polypropylene tubes and preserved at ≤4 °C during transport to the laboratory where they were frozen. Sub-samples for determination of suspended sediment concentration (not all events for Puarenga Stream, Table S1†) were collected in clean plastic bottles and analysed on return to the laboratory or refrigerated for up to five days.

A total of six separate periods were sampled for the Ngongotaha Stream and 13 for the Puarenga Stream (Fig. 3). Two distinct Q peaks were sampled during Puarenga Stream sampling of 11–15 May 2010 (event # 1 and # 2, Fig. 3), hence, a total of 14 separate events with distinct hydrograph peaks were sampled on this stream. During three events, both streams were sampled simultaneously (two in late Austral summer, one in winter; Fig. 3) to specifically study how pollutant transport varied between the two streams during the same rain events and similar antecedent hydrological conditions. In total, there were three gaps >3 h during sampling due to sampler malfunction or maintenance periods, none of which occurred during Q_{max} (Table S1†). Two grab samples (in duplicate) were also collected
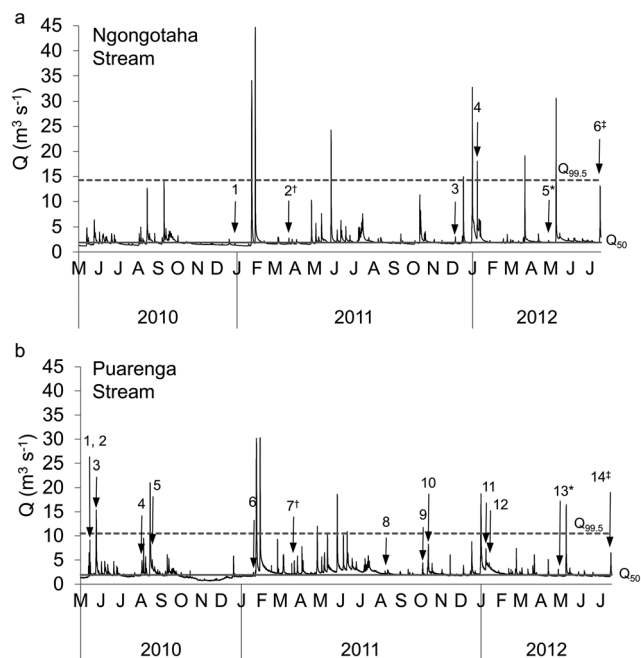
Fig. 3 Hourly measured discharge (Q) in the Ngongotaha (a) and Puarenga (b) streams during May 2010–August 2012. Solid horizontal line denotes median discharge (Q_{50}) and dashed line denotes the 99.5 discharge percentile ($Q_{99.5}$). Numbers denote sampling periods (Table S1†), superscript symbols denote events for which both streams were simultaneously sampled.

during a large event in August 2012 (Ngongotaha Stream $Q = 22.0$ m³ s⁻¹, Puarenga Stream $Q = 10.8$ m³ s⁻¹) and data (TN, TP and TSS concentrations) were used in derivation of regression models (see below).

Water quality analysis

Sediment concentrations were determined by filtering 65–500 mL of stream water through pre-combusted (550 °C for 3 h) and pre-weighed glass fibre filters (0.5 μm, Advantec GF GC-50). Total suspended sediment (TSS) concentrations were determined gravimetrically following drying (105 °C for 8 h) and volatile suspended sediment (VSS) concentrations were then determined by weight difference following subsequent ashing (550 °C for 3 h). Dissolved nutrients (NH₄, NO₂, NO₃, PO₄) were measured with an Aquakem 200 discrete analyser (Thermo Fisher) using standard colorimetric methods.[34] Limits of detection were 0.001 mg N L⁻¹ for NO₂, NO₃, 0.002 mg N L⁻¹ for NH₄ and 0.001 mg P L⁻¹ for PO₄. Total nitrogen (TN) and total phosphorus (TP) concentrations were determined following alkaline persulphate digestion[34] of an unfiltered sample and subsequent colorimetric analysis for NO₃ and PO₄ respectively, using a Lachat QuickChem flow injection analyser (Zellweger Analytics Inc.). Total dissolved nitrogen (TDN) and total dissolved phosphorus (TDP) concentrations were determined as for TN and TP respectively but using the field-filtered sample (0.5 μm, Advantec GF GC-50). These last two analyses were only undertaken for the three events when both streams were simultaneously sampled.

Data treatment and measured load calculation

Dissolved organic nitrogen (DON) concentration was determined as TDN minus the sum of NH₄–N, NO₂–N and NO₃–N; dissolved organic phosphorus (DOP) was determined as TDP minus PO₄–P. A value of zero was assigned when concentrations of DON and DOP were below the limit of detection. A small number (<5%) of concentration data were disregarded due to suspected contamination arising from sampling or measurement error (e.g. when PO₄–P > TP). For load calculations, disregarded concentration values were replaced with the mean of the two hourly measurements immediately before and after the anomalous result. Such estimated values are not reported.

Daily loads of determinands during each storm event were calculated using samples collected during the 24 h period of maximum Q that was continuously sampled. The approximate duration of events was one day and loads were calculated for standard 24 h periods (rather than the duration of individual events) primarily to aid comparison between streams and events. It also negated the need to fill gaps in concentration data for the minority of events which were not completely sampled or for which there were breaks in sampling. Observed 24 h loads were calculated as:

$$L = \sum_{i=1}^{n} \left(\frac{C_i + C_{i-1}}{2} \right) \left(\frac{Q_i + Q_{i-1}}{2} \right) \quad (1)$$

where L is the calculated 24 h load (kg per day), n is the number of samples collected during the 24 h period and C_i and Q_i are determinand concentration and discharge respectively at time i.

Consequently, event mean concentration (24 h EMC) of determinands was calculated as:

$$24 \text{ h EMC} = \frac{24 \text{ h load}}{\sum_{i=1}^{n} \left(\frac{Q_i + Q_{i-1}}{2} \right)} \quad (2)$$

Quantifying hysteresis in concentration–Q relationships

Scatter plots of relationships between determinand concentration and Q for each event (typically the entirety of the sampling period) were inspected to identify hysteresis that reflected consistent difference in concentration between the rising and recessing limbs of the hydrograph. Observed hysteresis was subsequently characterised for all sampling periods that included at least five samples collected during both the rising and recessing limbs of the hydrograph. Hysteresis was quantified by fitting two parameters (p and g) to the following model proposed by Bowes et al.[17] after House and Warwick.[18]

$$\hat{c}_i = C_{base} + p \left(\frac{Q_i - Q_{i-1}}{dt} \right) + \frac{(g(Q_i - Q_{base}))}{Q_i Q_{base}} \quad (3)$$

where $\hat{c}_i$ is estimated determinand concentration (mg L⁻¹) at time i, C_{base} is the mean determinand concentration (mg L⁻¹) measured in samples collected during the sampling period prior to the onset of the hydrograph rising limb, dt is time elapsed (s) between times i and $i - 1$ and Q_{base} is the mean discharge (m³ s⁻¹) during the sampling period prior to the onset of the hydrograph rising limb. Parameter p is a response factor

$(g\ m^{-6}\ h^2)$ that quantifies the magnitude of the hysteresis loop, as well as the direction, *i.e.* clockwise ($p > 0$, concentration higher during rising limb than the recessing limb) or anti-clockwise ($p < 0$, *vice versa*). Parameter g is a loop gradient term $(g\ s^{-1})$ that is related to the size of the hydrograph peak and is normalised with respect to Q. Both p and g were determined by iteration using the Solver add-in to Microsoft Excel 2007 with the objective to minimise the root mean squared error between measured (C_i) and estimated concentration ($\hat{c}_i$) during the sampling period.

Comparison of load estimation methods

The extensive dataset collected during this study provided an opportunity to compare the accuracy of a range of commonly used methods for estimating pollutant loads. Observed 24 h loads of TN, TP and TSS were compared to estimates derived using the following three main methods of load estimation:[35] averaging, ratio estimation and regression approaches.

Averaging approaches are frequently used when few concentration data are available. The Bay of Plenty Regional council conduct routine (monthly) monitoring, which furnishes a time series of monthly concentrations. An important question is whether event loads can be estimated accurately as the product of Q measured continuously during a storm event and the mean concentration of samples collected during routine monitoring. Event pollutant loads were thus estimated from the product of Q measured hourly during a storm event and the mean concentration of routine samples:

$$L_{avg} = \overline{C}_{monthly} \times \sum_{i=1}^{n} Q_i \qquad (4)$$

where L_{avg} is the estimated 24 h event load and $\bar{C}_{monthly}$ is the mean concentration of 20–25 grab samples collected at approximately 4 week intervals by the regional council between May 2010 and July 2012 as part of a routine monitoring programme. The Ngongotaha Stream site was ≈ 1 km downstream from the event sampling site and the Puarenga Stream sites were at the same location.

Ratio estimation methods assume correlation between concentration and an auxiliary variable which is more frequently sampled (typically Q).[35] Instantaneous load estimates are consequently proportionally adjusted with reference to the auxiliary variable to derive a load for longer time periods, *e.g.* greater weighting is apportioned to concentration measurements taken when Q is high. To reflect correlation between concentration and Q, the Q-weighted mean concentrations were calculated using data collected in this study, and used in place of the arithmetic means of eqn (4). To maintain independence, Q-weighted mean concentrations were calculated separately for each load calculation using only data for other events.

$$C_{QWM} = \frac{\sum_{j=1}^{N} C_j Q_j}{\sum_{j=1}^{N} Q_j} \qquad (5)$$

where C_{QWM} is the discharge-weighted mean concentration, N is the number of samples and C_j and Q_j are determinand concentration and discharge respectively measured during sampling periods at time j. Then:

$$L_{ratio} = C_{QWM} \times \sum_{i=1}^{n} Q_i \qquad (6)$$

where L_{ratio} is the estimated 24 h event load.

Regression can be used to estimate concentration based on Q (rating curves) where a defined relationship exists between the two variables and when data relating to a sufficiently wide range of Q are available.[8] $\log_{10}$–$\log_{10}$ rating curves were constructed using ordinary least squares linear regression and loads estimated as:

$$L_{rating} = \sum_{i=1}^{n} \left(\frac{\hat{C}_i + \hat{C}_{i-1}}{2} \right) \left(\frac{Q_i + Q_{i-1}}{2} \right) \qquad (7)$$

where L_{rating} is the estimated 24 h load and $\hat{C}_i$ is concentration at time i estimated with a rating curve constructed using only data measured during other sampling periods. All dependent variables used in regression models were $\log_{10}$-transformed and untransformed estimators were derived by calculating the antilogarithm and multiplying by the following bias correction factor (BCF) proposed by Ferguson:[36]

$$BCF = e^{2.65\sigma^2} \qquad (8)$$

where σ^2 is the model variance.

In addition to Q, other hydrological variables that affect pollutant transport have been shown to explain additional variation in concentration measurements.[16] Regression models were trialled that used the following independent variables to predict measured concentration: $\frac{Q_i}{Q_{i-x\ h}}$ where $Q_{i-x\ h}$ is discharge x h prior to sampling (values for x of 1, 1.5, 2 and 3 were considered); the sum of rainfall measured in preceding 1, 3 and 6 h, and soil moisture (%) at the time when the sample was collected. Linear interpolation of hourly measurements was used to derive sub-hourly estimates of independent variables.

Additional hydrological variables aside from Q were only used to improve prediction of TN and TP concentrations for the Puarenga Stream, as datasets for this stream were the most extensive, and included events during different seasons with a range of different characteristics. The aim when trialling regression models was to seek parsimonious compromise between maximising model performance (r^2) and minimising the number of independent variables. Where necessary, variables were transformed to improve normality and ensure linearity of relationships. Residual plots were visually inspected for normal distributions. The predictive power of the TN model for the Puarenga Stream was improved with the addition as an independent variable of the ratio of Q at the time of sampling to Q 3 h previously ($Q_i/Q_{i-3\ h}$):

$$\widehat{TN}_{hydrol} = (\beta_1 \times \log_{10} Q_i) - \left(\beta_2 \times \left(\frac{Q_i}{Q_{i-3\ h}} \right) \right) + c_1 \qquad (9)$$

where $\widehat{TN}_{hydrol}$ is estimated $\log_{10}$ transformed TN concentration, β_1 and β_2 are regression coefficients (both > 0) and c_1 is the y intercept of the regression line.

The predictive power of the TP model for the Puarenga Stream was improved with the addition of the following independent variables: the ratio of Q at the time of sampling to Q 1.5 h previously ($Q_i/Q_{i-1.5\ h}$); the sum of rainfall (mm) in the preceding 6 h ($\log_{10}$ + 1 transformed; $rain_6$), and soil moisture (%) at the time of sampling (square-root transformed; soil):

$$\widehat{TP}_{hydrol} = (\beta_3 \times \log_{10} Q_i) - \left[\beta_4 \times \left(\frac{Q_i}{Q_{i-1.5\ h}} \right) \right] + (\beta_5 \times rain_6) - (\beta_6 \times soil) + c_2 \qquad (10)$$

where $\widehat{TP}_{hydrol}$ is estimated $\log_{10}$ transformed TP concentration, β_3, β_4, β_5, and β_6 are regression coefficients (all > 0) and c_2 is the y intercept of the regression line.

Regression coefficients and y intercept values were determined using ordinary least squares linear regression. To maintain independence, values for these parameters were determined individually for each event using only measured data for all *other* events.

Consequently, estimated loads (L_{hydrol}) were calculated using eqn (1) with substitution of C_i for concentration estimated using regression models described above that included two or more hydrological variables as predictors.

Quantifying temporal inequality in pollutant transport

In order to compare how determinand loading varied temporally between the two streams over longer time periods, regression models fitted to measured data (see above) were used to estimate the average hourly concentration of TN, TP and TSS in each stream over the two-year period of May 2010–May 2012 (soil moisture probe malfunctioned in June 2012). Root mean squared error statistics were calculated for models using a bootstrapped sample drawn from measured data (sample with replacement; $n = 10\ 000$). Lorenz curves were then constructed to examine how the cumulative proportion of the total estimated two-year load (x) varied with respect to the cumulative proportion of time (y). The Gini coefficient (G) was calculated to quantify temporal inequality in loading; this parameter equals the ratio of the area enclosed by the Lorenz curve and the 1 : 1 line, to the area under the 1 : 1 line (Fig. 1). The parameter therefore equals a value between 0 (loading is equal at all times) and 1 (all loading occurs in an infinitesimally small period). For constructed Lorenz curves, G was calculated as:

$$G = 1 - 2 \int_0^1 Y(X) \mathrm{d}X \qquad (11)$$

with integration performed numerically.

Results

Hydrology

The sampling periods spanned a wide range of Q (Fig. 3). Although median Q was very similar in the two streams

(≈ 1.9 m^3 s^{-1}) the hydrograph for the Puarenga Stream (highest circularity ratio and drainage density) was the flashier of the two, with more peaks and steeper base flow recession. By contrast, the Ngongotaha Stream hydrograph displayed fewer peaks but higher Q_{max} during large storms (*e.g.* $Q_{99.5}$ was highest in the Ngongotaha Stream, Fig. 3). Discharge during the study period exceeded the range of sampled Q for 0.35% of the total time for the Puarenga Stream and for 0.25% of the time for the Ngongotaha Stream. Rainfall was above average during the sampling period; *e.g.*, total rainfall for Rotorua city was 6% above the 1981–2010 average in 2010 (1436 mm) and 47% above average in 2011 (1997 mm).[37] In particular, uncharacteristically high rainfall occurred during both Austral summers and two very large floods occurred in January 2011 following passage of tropical anticyclones, although these were not sampled. Hourly Q_{max} in the Ngongotaha Stream during the largest flood was the highest measured for 15 years[38] (long-term continuous monitoring data not available for the Puarenga Stream).

Relationships between concentration and discharge

Data for the three events during which both streams were sampled illustrate typical relationships between determinand concentration and Q (Fig. 4–6). Suspended sediment concentrations were highly positively correlated with Q in both streams (*e.g.* Fig. 4b and f). Suspended sediments were predominantly inorganic; on average VSS comprised 32% of TSS sampled in the Puarenga Stream and 42% in the Ngongotaha Stream. The proportion of TSS comprising VSS varied widely between events at base flows, although it was typically $\approx 20\%$ during storm flow in both streams indicating relatively higher flux of inorganic sediments during storm events.

Concentrations of NO_3 typically exhibited a weak dilution effect in both streams and declined during the period of Q_{max} (*e.g.* Fig. 5c and d). Consequently, the lowest NO_3–N 24 h EMCs measured in the Ngongotaha Stream occurred during the largest events (events # 4 and # 6; Table S1†). During the recessing limb of the hydrograph, an increase in NO_3–N concentrations to above pre-event base flow was observed in several events sampled in the Puarenga Stream (*e.g.* Fig. 5g). Total nitrogen concentrations were positively correlated with Q in both streams although this determinand was invariant during smaller events as a result of minor increases in concentrations of DON and particulate N being balanced by reduced NO_3–N concentrations (*e.g.* Fig. 4c). Concentrations of NH_4–N typically comprised only a small proportion of TN concentrations (Ngongotaha Stream mean = 2%; Puarenga Stream mean = 9%) and generally showed no clear relationship with Q, although highest concentrations were measured during the largest events in both streams. Concentrations of NO_2–N were less than detection limits (<0.001 mg L^{-1}) in all samples and are not presented.

Concentrations of PO_4 were highly variable; coefficients of variation for this determinand in the streams were 43% (Ngongotaha) and 56% (Puarenga). Typically, concentrations of PO_4–P during events were a minor component of TP concentrations and unrelated to Q, although the March 2011 event
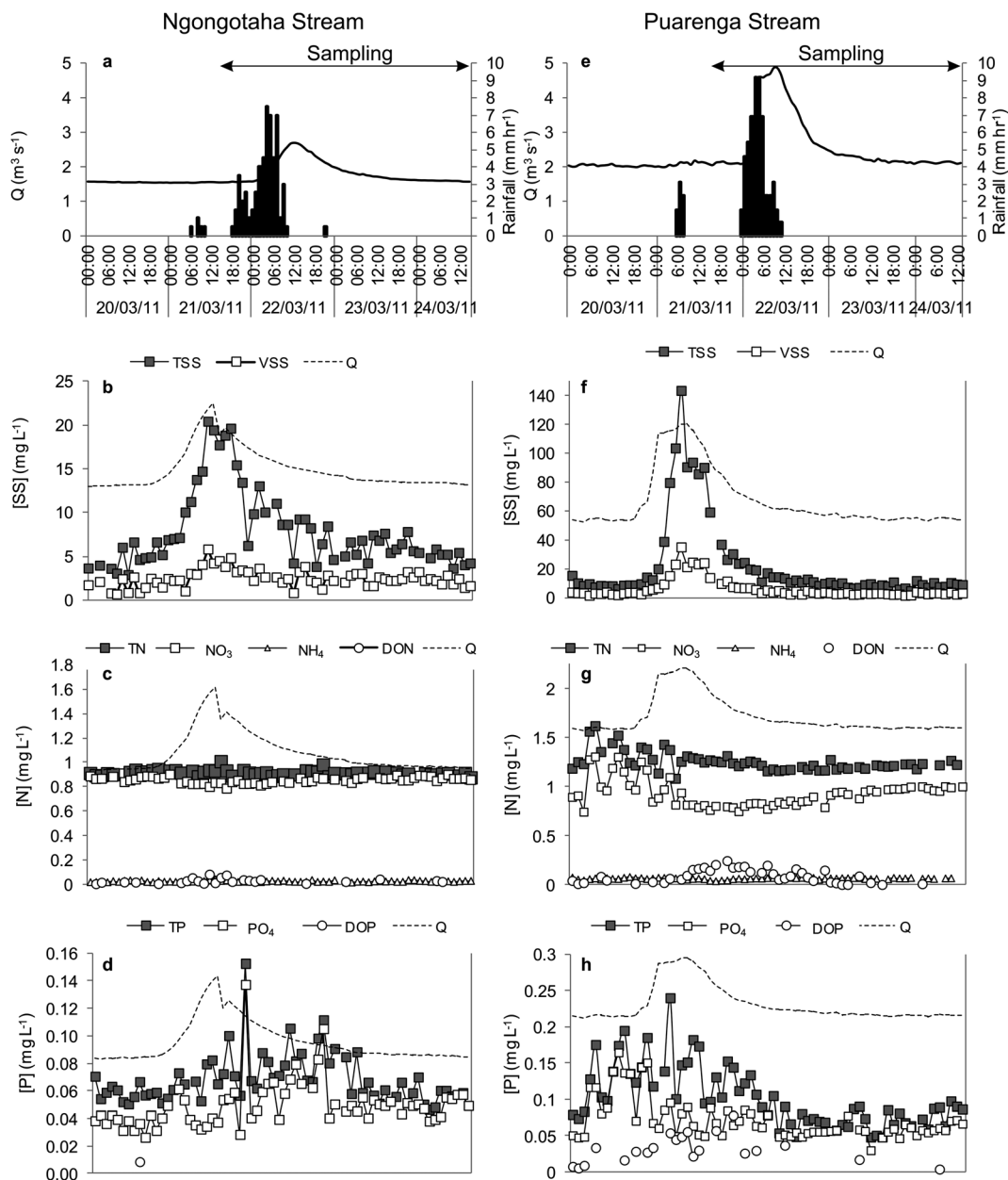
Fig. 4 Temporal variations in measurements for the Ngongotaha Stream (left panels, (a–d)) and the Puarenga Stream (right panels, (e–h)) during simultaneous sampling of both streams in March 2011 (event # 2 and # 7 respectively; Fig. 3). Scale for discharge (Q) data not shown on concentration plots.

(medium-sized event in late summer) during which both streams were sampled was an exception as PO_4–P concentrations displayed peaks after and before Q_{max} respectively in the Ngongotaha and Puarenega streams (Fig. 4d and h). Total P concentrations exhibited positive correlation with Q in both streams (*e.g.* Fig. 5d and 5h). The relative rate at which concentrations of TP increased with Q was typically greater than for TN, hence, mass ratios of TN : TP generally decreased during storm flow. Dissolved organic P was a minor component of the TP pool in the three events for which it was measured (Fig. 4d, h, 5d, h, 6d and h) and the positive correlation between TP concentrations and Q therefore overwhelmingly reflects mobilisation of particulate P during elevated Q.

Hysteresis in concentration–discharge relationships

Temporal trends in determinand concentration during events were not always aligned with variations in Q. For example, marked increases in concentrations of TN and TP in the Puarenga Stream (due to peaks in NO_3 and PO_4 respectively) observed at the start of event # 7 occurred following very light rainfall that had negligible influence on Q, thereby suggesting flushing of local pollution sources (Fig. 4g and h). Similarly, TP concentrations in the Puarenga Stream display a distinct local peak during event # 14 approximately 16 h before Q_{max} (Fig. 6h), consistent with apparent flushing of TSS (Fig. 6f).
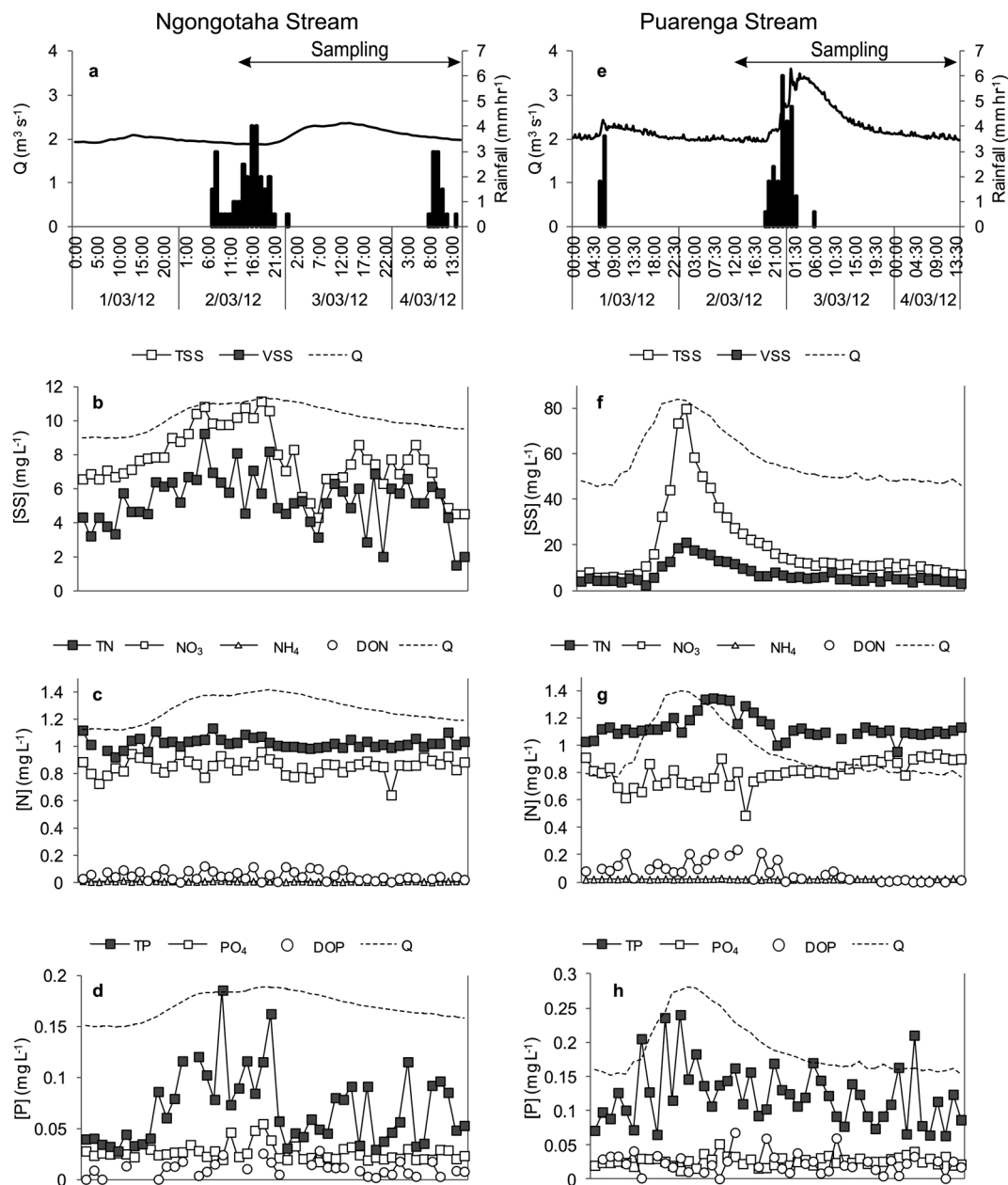
Fig. 5 Temporal variations in measurements for the Ngongotaha Stream (left panels, (a–d)) and the Puarenga Stream (right panels, (e–h)) during simultaneous sampling of both streams in March 2012 (event # 5 and # 13 respectively; Fig. 3). Scale for discharge (Q) data not shown on concentration plots.

Calculation of the response factor (p) and loop gradient term (g) allowed such hysteretic behaviour in concentration–Q relationships to be quantified (Table S2†). Fig. 7 shows examples of observed hysteresis in four determinands and illustrates relative differences between hysteresis loops with various values for p and g. Observed hysteresis in TN in the Puarenga Stream was always anticlockwise (*i.e.* $p < 0$; Fig. 7a) indicating relatively elevated concentrations during the recessing limb, an occurrence that usually reflected elevated NO_3–N measured post Q_{max} as recessing Q approached pre-event levels. Of the two examples of hysteresis in TN observed in the Ngongotaha Stream, one was small ($g = 2.97$ g s^{-1}) and clockwise ($p > 0$; Fig. 7a), the other anticlockwise. Both clockwise and anticlockwise hysteresis in TP was observed in the Puarenga Stream and the largest TP

hysteresis loops ($g = 0.51$–0.97 g s^{-1}) observed in the Puarenga Stream were anticlockwise (*e.g.* Fig. 7b). Various hysteresis patterns were observed for TSS during all three events when both streams were concurrently sampled. For example, anticlockwise hysteresis was observed in both streams in the March 2011 event (medium-sized event in late summer; Fig. 4b and f), whereas clockwise hysteresis was observed for TSS in both streams during the July 2012 event (larger event in winter; Fig. 6b, f and 7c).

Storm load size and composition

During similar Q, TN, TP and TSS concentrations were typically lower in the Ngongotaha Stream (*e.g.* see 24 h EMCs in Table S1†) and therefore loads during similar-sized events were
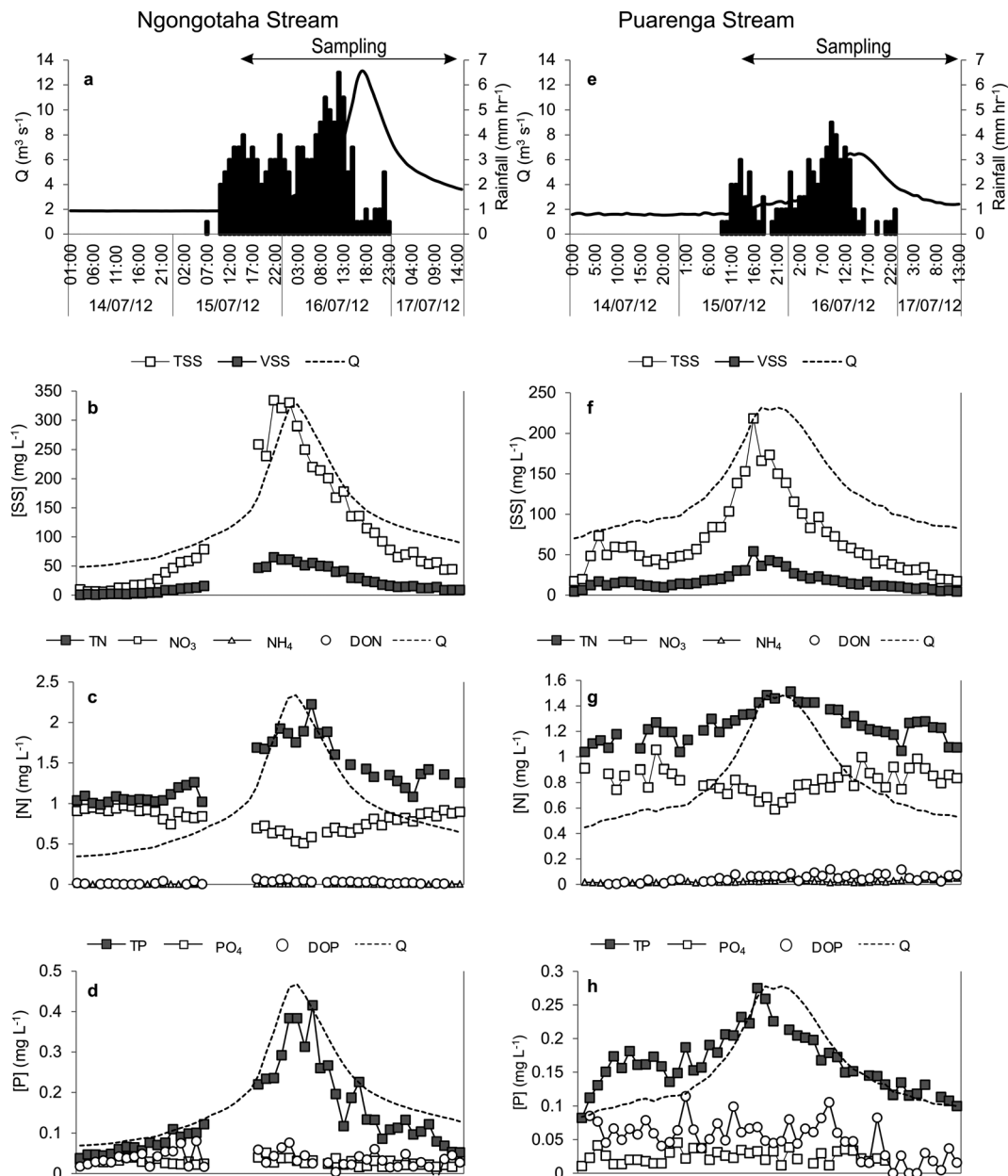
Fig. 6 Temporal variations in measurements for the Ngongotaha Stream (left panels, (a–d)) and the Puarenga Stream (right panels, (e–h)) during simultaneous sampling of both streams in July 2012 (event # 6 and # 14 respectively; Fig. 3). Scale for discharge (Q) data not shown on concentration plots. There was a 7 h break in sampling (sampler malfunction) during the rising limb for Ngongotaha Stream data.

higher for the Puarenga Stream. Comparison of 24 h loads highlights large disparities between events of different magnitude that result from the positive correlation between determinand concentration and discharge (Fig. S1†). The largest measured 24 h loads of TN, TP and TSS for the Ngongotaha Stream were, respectively 9, 23 and 220 times greater than the smallest loads. For the Puarenga Stream, the largest measured 24 h loads of TN, TP and TSS were, respectively, 10, 9 and 10 times greater than the smallest loads.

Measured 24 h loads in the Ngongotaha Stream (Fig. S1†) were higher for event # 6 ($Q_{max} = 13.1$ m^3 s^{-1}) than event # 4 ($Q_{max} = 18.0$ m^3 s^{-1}) because, despite higher Q_{max}, the

cumulative Q was 21% lower for event # 4 during which only the rising limb and peak of the hydrograph were sampled (sampler was removed shortly after Q_{max} to remove risk of damage to the instrument).

The relative contribution of dissolved inorganic nutrients to TN and TP loads decreased with increasing Q (Fig. S1a–e†). This was particularly the case for TP; the contribution of PO$_4$–P to measured 24 h loads of TP varied from 12% ($Q_{max} = 13.1$ m^3 s^{-1}) to 66% ($Q_{max} = 2.7$ m^3 s^{-1}) in the Ngongotaha Stream and from 11% ($Q_{max} = 5.0$ m^3 s^{-1}) to 55% ($Q_{max} = 4.8$ m^3 s^{-1}) in the Puarenga Stream. The majority of measured 24 h TN loads comprised predominantly dissolved inorganic N (Ngongotaha
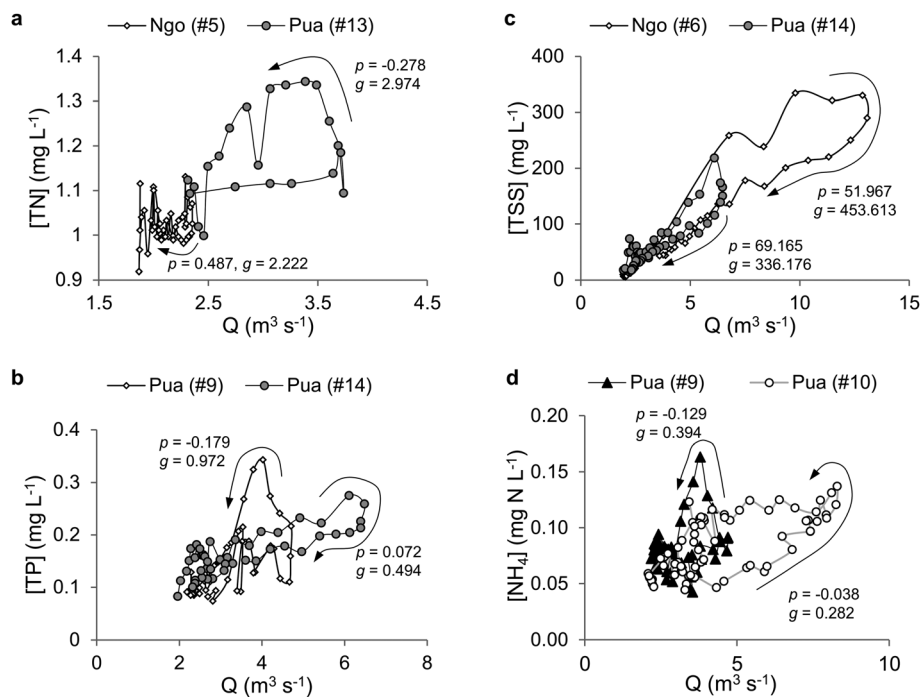
Fig. 7 Examples of hysteresis loops in measured concentrations of total nitrogen (TN), total phosphorus (TP), total suspended sediments (TSS) and ammonium (NH$_4$) for the Ngongotaha (Ngo) and Puarenga (Pua) streams. Parameter p is a response factor (g m^{-6} h^2) that quantifies the magnitude of the hysteresis loop, as well as the direction, *i.e.* clockwise ($p > 0$, concentration higher during rising limb than the recessing limb) or anti-clockwise ($p < 0$, *visa versa*). Parameter g is a loop gradient term (g s^{-1}) that is related to the size of the loop.

Stream range = 43–89%; Puarenga Stream range 57–82%), and the contribution of dissolved inorganic N to 24 h TN loads was less than 50% in only the two largest events sampled on the Ngongotaha Stream. Loads of NH$_4$–N were typically minor compared to NO$_3$–N loads although event # 3 for Puarenga Stream (autumn event with highest stream Q_{max} sampled) was an exception: approximately 20% of the 24 h TN load comprised NH$_4$–N (Fig. S1d†) and NH$_4$–N 24 h EMC (0.498 mg L^{-1}; Table S1†) was approximately an order of magnitude greater than for other events sampled. Measurements of DON (Fig. 4c, g, 5c, g and 6c, g) indicated that this fraction comprised a larger proportion of the TN in event loads transported in the Puarenga Stream (largely forested catchment) than in the Ngongotaha Stream. Loads of DON in the Puarenga Stream, expressed as a proportion of the 24 h TN loads, were 9% (event # 7), 27% (event # 13) and 20% (event # 14), whereas for the Ngongotaha Stream, DON comprised 3% (event # 2), 9% (event # 5) and 11% (event # 6) of the 24 h TN loads. Similarly, the relative contribution of DOP to 24 h TP loads was also highest in the Puarenga Stream. Proportions in the Puarenga Stream were 24% (event # 7), 17% (event # 13) and 30% (event # 14), compared to 0%, 14% and 15% in the Ngongotaha Stream.

Suspended sediment loads during events predominantly comprised inorganic sediments (*e.g.* Fig. 4b and f). The relative contribution of VSS to 24 h TSS loads was similar in both streams ($\approx$ 15 to 30%), although an atypically large proportion of the 24 h TSS load comprised VSS (69%) for Ngongotaha Stream event # 5, suggesting flushing of organic material accreted during the dry period prior to this very small event during late summer.

Comparison of load estimation methods

Table S3† presents comparison between estimated and measured 24 h loads. Measured loads are calculated using eqn (1). Estimated loads are calculated using one averaging method (L_{avg}; eqn (4)), one ratio method (L_{ratio}; eqn (6)) and two regression methods (L_{rating}; eqn (7) and L_{hydrol}).

The averaging method (that used mean concentrations of samples collected during routine monthly monitoring) substantially underestimated measured 24 h loads for TP, TN and TSS, as routine monitoring was typically conducted during base flow when TP, TN and TSS concentrations were lower than during storm events.

The ratio estimation method yielded imprecise loads (*e.g.* −61% to +183% error for TP loads). However, it generally yielded more accurate 24 h TN loads than the averaging method for the largest events. Of the regression methods, L_{hydrol} was generally more accurate than L_{rating}, reflecting the inclusion of more independent variables (and subsequent higher predictive power) in models used to derive concentration estimates for L_{hydrol} calculations. Differences between TN L_{hydrol} and TN L_{rating} were, however, minor.

Temporal inequality in sediment and nutrient loading

Regression models fitted to measured hydrological variables and concentrations of TN, TP and TSS (Table S4†) were used to estimate cumulative hourly loads over the two-year period of May 2010–May 2012. All models included Q as an independent variable with positive coefficient, reflecting the positive

correlation between the three determinands and Q. Eqn (9) and (10) were used to estimate concentrations of TN and TP respectively in the Puarenga Stream, as the inclusion in these models of hydrological variables in addition to Q_i improved predictive power. Regression coefficients and y intercept values for these equations were fitted using all measured data (see Table S4† for full equations). Given the high number of independent variables in the TP model, there was uncertainty about the validity of extrapolating to periods when antecedent hydrological characteristics deviated markedly from those during sampling. Consequently, a linear $\log_{10}$–$\log_{10}$ rating curve was used to estimate TP concentration based on Q_i for periods when estimated TP concentration exceeded the maximum that was measured (0.543 mg L^{-1}; 4% of time period). Linear $\log_{10}$–$\log_{10}$ rating curves with high r^2 values (0.72 and 0.68 respectively) were used to estimate measured TN and TP concentration for the Ngongotaha Stream. A linear $\log_{10}$–$\log_{10}$ rating curve was used to estimate TSS concentration in the Puarenga Stream although a marginally poorer-fitting power function (exponent < 1) was used to estimated TSS concentration when Q exceeded the Q_{max} during TSS sampling (10.81 m^3 s^{-1}; 0.6% of time period) in order to minimise likelihood of over-estimating concentration during high Q periods which contribute disproportionally to cumulative load. Similarly, a power function with exponent <1 provided good approximation of measured TSS concentration in Ngongotaha Stream samples and was applied to the measured Q range. Maximum estimated concentrations (mg L^{-1}) of TN, TP and TSS, relative to maximum measured concentrations (in parentheses), for the two-year period were 2.78 (2.75), 0.788 (0.427) and 2250 (510.46) respectively in the Ngongotaha Stream and 2.58 (3.096), 0.542 (0.543) and 682.46 (462.54) respectively in the Puarenga Stream.

Plotting cumulative estimated loads as a function of cumulative time allowed temporal inequality in pollutant loading over the two-year period (May 2010–May 2012) to be examined (Fig. 8). Gini coefficients for individual determinands were ordered as follows in both streams: TN < TP < TSS. Temporal inequality in loading was therefore lowest for TN and highest for TSS, *i.e.* a given proportion of the TSS total load was transported to the lake in a shorter time than the same proportion of the TN load when estimated hourly loads are arranged in order of increasing magnitude and the largest loads are considered. The value of G for TN was the same in both streams (0.312) indicating, for example, that 50% of the TN load in both streams was transported in approximately 28% of the time (expressed as days in Table 1; minor difference between catchments reflects rounding of G). Gini coefficients for TP and TSS were highest for estimates of loads conveyed in the Ngongotaha Stream; 50% of estimated TP loading occurred for 10% of time for the Ngongotaha Stream ($G = 0.511$), compared to 17% of time for the Puarenga Stream ($G = 0.455$). Extremely high inequality for TSS load estimates implies that 50% of the total TSS load over the two-year period was estimated to have been transported in a cumulative time equivalent to approximately just 1 day for the Ngongotaha Stream ($G = 0.909$) and 7.5 days for the Puarenga Stream ($G = 0.793$). Expressing G in terms of
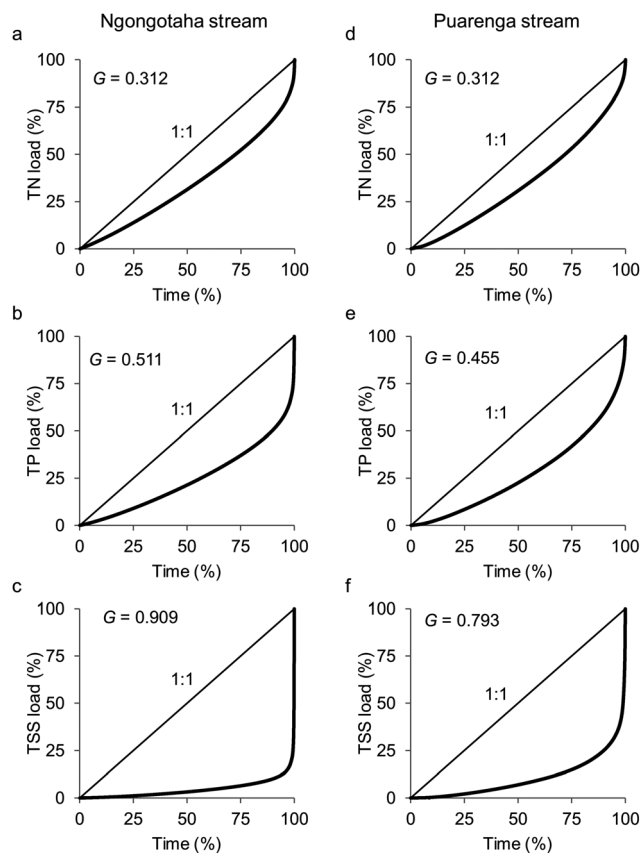

Fig. 8 Lorenz curves describing the relationship between cumulative proportion of estimated hourly loads during two-years (May 2010–May 2012) and cumulative proportion of time for the Ngongotaha (a–c) and the Puarenga (d–f) streams. Gini coefficients (G) quantify temporal inequality in loading (see Fig. 1 for calculation method). TN, total nitrogen; TP, total phosphorus; TSS, total suspended sediments.

days aids interpretation although it is important to note that one 'day' may, for example, comprise 24 separate 1 h periods during Q_{max} of 24 events.

Yield estimates

Two-year load estimates derived using regression models to estimate concentration (see above) were used to estimate yields of TN, TP and TSS from each stream surface catchment on a per

Table 1 Estimated shortest time (nearest 0.5 day) during which 25% and 50% of the total loads of total nitrogen (TN) total phosphorus (TP) and total suspended sediment (TSS) were conveyed in the Ngongotaha and Puarenga streams during a two-year period (May 2012–May 2012). Estimates are based on modelled hourly loads and 'days' do not necessarily comprise consecutive hours

| Proportion of cumulative load | Time (days) | | | | | |
| | Ngongotaha Stream | | | Puarenga Stream | | |
	TN	TP	TSS	TN	TP	TSS
50%	201.5	75.5	1.0	206.5	126.0	7.5
25%	41.5	3.5	0.5	57.5	23.0	1.5

Table 2 Estimated yields of total nitrogen (TN), total phosphorus (TP) and total suspended sediment (TSS) from the Ngongotaha and Puarenga surface stream catchments. Yields are based on estimated loads during May 2010–May 2012. Yields are calculated with and without (discharge during 23/01–01/02 replaced with median values) inclusion of the two large floods in January 2011 (see Fig. 3)

Stream catchment	January 2011 storms included?	Yield (kg ha^{-1} yr^{-1})		
		TN	TP	TSS
Ngongotaha	Y	12.73	1.01	741
	N	11.90	0.90	359
Puarenga	Y	12.71	1.34	479
	N	12.00	1.22	330

unit area basis (Table 2). Estimated yields of TN were very similar for the catchments (≈ 12.7 kg ha^{-1} yr^{-1}) while TP yield was approximately 30% higher in the Puarenga Stream catchment (1.34 kg ha^{-1} yr^{-1}) compared to the Ngongotaha Stream catchment (1.01 kg ha^{-1} yr^{-1}). Estimated yield of TSS was markedly greater in the Ngongotaha Stream catchment (741 kg ha^{-1} yr^{-1}) compared to the Puarenga Stream catchment (479 kg ha^{-1} yr^{-1}). This difference can, however, be attributed largely to the occurrence of larger peak Q during the two flood events in January 2011; TSS yield estimates made without inclusion of the flood peaks (substitution of Q_{50} for the nine-day period) are comparable for the two catchments (≈ 350 kg ha^{-1} yr^{-1}). These large events were not sampled and, consequently, contribute considerable uncertainty to load estimates.

Discussion

Summary

By analysing data for >900 samples collected during 17 hydrological events, this study provides insight into how hydrological and catchment characteristics interact to influence sediment and nutrient transport across landscapes. High-frequency sampling during a wide range of discharge (Q) enabled relationships between Q and concentrations of various suspended sediment and nutrient fractions to be determined. Quantification of hysteretic behaviour in these relationships provided information about likely relative importance of far- *versus* near-channel sources during individual events. Lastly, quantification of temporal inequality in loading highlighted the importance of considering storm flow processes in loading estimates and emphasised the potentially highly disproportionate contribution of individual flood peaks to estimates of annual-scale loads for a nationally iconic lake.

Temporal variations in nutrient and suspended sediment concentration during events

The relationships between concentration and Q for individual determinands were broadly similar between the two streams. The observed decreases in NO$_3$–N concentration during storm flow can be attributed to dilution by rainfall of steady inputs to the stream channels from groundwater sources high in NO$_3$. Studies elsewhere have similarly reported dilution of NO$_3$ following onset of storm flow, typically followed by increases in

NO$_3$ to above pre-event concentrations,[14,39,40] as was frequently observed in data for the Puarenga Stream. In general though, maximum observed post-event increases in NO$_3$ were relatively modest (*e.g.* $\approx 25\%$ above pre-event NO$_3$–N for Puarenga Stream event # 10); by contrast, Vanni *et al.*[39] report up to five-fold increases in NO$_3$–N concentrations for the recessing limb in a stream draining a predominantly arable catchment, while Oeurng *et al.*[41] report increases in NO$_3$ from approximately 8 mg N L^{-1} to > 30 mg N L^{-1} in a large French river, even after small events. Such behaviour likely reflects diffuse delivery of NO$_3$ to the stream channel by through flow processes and accounts for the anticlockwise hysteresis in NO$_3$ observed during several events for the Puarenga Stream (but not the Ngongotaha Stream) (Table S2†). This result also accounts for the significance of $Q_i/Q_{i-3\text{ h}}$ as an independent variable (negative coefficient) in the regression model used to predict TN concentrations for the Puarenga Stream.

The lack of relationship between concentrations of PO$_4$–P and Q that was generally observed conforms to the 'Type 1' classification proposed by Haygarth *et al.*[42] who note that such behaviour likely reflects occurrence of steady state between the dissolution kinetics of the soil and stream water. The coarse volcanic soils in the lake catchment are high in allophanic clays which have high capacity to adsorb phosphorus[43] and, therefore, stream sediments likely buffer PO$_4$ in stream water *via* either adsorption or desorption processes.[44] When either peaks or hystereses in PO$_4$–P were apparent, they were typically during small events (*e.g.* Table S2†, Fig. 4d) or outside of the period of storm flow (*e.g.* Fig. 4h). It is possible, therefore, that ratios of TSS to PO$_4$–P were insufficient during these periods to readily buffer elevated PO$_4$–P arising from flushing processes.

The strong positive relationship between concentrations of TP and Q has been observed elsewhere[14,45,46] and generally reflected mobilisation of inorganic particulate phosphorus (PP) by erosive processes during storm flow. Consequently, concentrations of TSS and TP were highly correlated (*e.g.* compare Fig. 6f and h) and, where observed, the direction of hysteresis with Q tended to be the same for both determinands suggesting similarity of sources. The importance of erosive processes in determining TP variations is reflected in the inclusion of both rainfall and soil moisture content (positive coefficients) as independent variables in the regression model used to predict TP concentrations for the Puarenga Stream; both these variables directly influence overland flow which is the dominant transport mechanism for PP across landscapes.[47] The strong correlation between TP and Q accounted for the frequent large underestimations in TP loads (more so than for TN) when using averaging methods based on samples predominantly collected during base flow periods (L_{avg}; Table S3†).

Concentrations of suspended sediments consistently increased with Q although some occurrence of hysteretic behaviour implied that variability in supply processes affected the linearity of this relationship.[19] Specifically, occurrence of clockwise hysteresis during larger events (*e.g.* Ngongotaha Stream event # 6; Fig. 7c) indicated depletion of within- or near-channel sediment sources (these two source areas cannot be distinguished), while anticlockwise hysteresis indicated delayed

delivery of sediments from far-channel sources to the stream channel (*e.g.* Puarenga Stream events # 7, # 8, # 9 and # 13; Table S2†).

Variations in nutrient and suspended sediment transport between catchments

Given the predominant land use in the two catchments, it is interesting to note that base flow concentrations of all N and P fractions were typically greater (although marginally so for PO_4) in the Puarenga Stream (mixed land use but predominantly forested) than in the Ngongotaha Stream (pasture dominated) since, relative to forested catchments, the occurrence of high nutrient concentrations in streams draining agricultural land is well established in New Zealand[48] and elsewhere.[49] In the case of N, it is noted that NO_3 was the main component of TN which, as discussed above, originates from groundwater sources. Therefore, due to discontinuity between surface and groundwater catchments that is present in the Lake Rotorua catchment,[27] groundwater chemistry does not necessarily reflect overlying land use. Furthermore, the large storage capacity of local aquifers means that mean residence time for nutrients in groundwater is in the order of decades (*e.g.* 16 years for the Ngongotaha Stream catchment[27]) and, therefore, the effects of current catchment land use are yet to be fully realised given the short time elapsed since agricultural intensification began in the lake catchment (mainly post-1940).[50] There is, however, evidence that recent nutrient-enrichment of the Ngongotaha Stream has occurred in conjunction with land use intensification; concentrations of NO_3–N measured when Q was below the median for the study period (0.84 mg L^{-1}, $n = 110$) were 60% higher than mean base flow NO_3–N reported by Hoare[51] for 1975–1978 (0.53 mg L^{-1}), a period since which substantial agricultural intensification has occurred in the stream catchment.[50] In addition, it is noted that there are numerous potential N sources in the Puarenga catchment, including naturally NH_4-enriched geothermal springs,[27] suburban land, farmland, and a wastewater application area where N-enriched treated effluent is spray irrigated (Fig. 2). Owing to the local free-draining soils, dissolved N in treated effluent has been shown to readily leach from experimental plots in the Puarenga catchment[52] and data following hydrological events do exhibit evidence of flushing in the catchment of both NH_4 and NO_3 that could potentially have originated from effluent sources (*e.g.* note unusually high NH_4–N 24 EMC following event # 3 and anticlockwise hysteresis for both determinands; Tables S1 and S2†). Methods used in this study cannot, however, be used to isolate the influence of individual sources, although data collected provide a comprehensive baseline to examine future trends and further assess potential environmental impacts of land management practices.

The higher TP concentrations generally measured in the Puarenga Stream reflect the typically higher TSS concentrations which, as discussed above, are a strong determinant of PP which was the dominant P fraction in samples. The relatively high TSS in the Puarenga Stream likely reflects the predominance of exotic forestry which has been shown to be related to elevated TSS in New Zealand streams; *e.g.* Quinn and Stroud[53] found that median TSS concentration (18.1 mg L^{-1}) in a stream draining a pine-forested catchment was the highest of seven sites with contrasting land use. Association between elevated TSS and exotic forestry can be attributed to the general lack of ground cover vegetation under plantation trees which promotes the formation of gully networks, the connectivity of which is a critical factor in influencing sediment transport in larger catchments (>10 km^2) where sediment flux tends to be transport- rather than supply-limited.[54] Plantation forest can also be associated with critical source areas such as unsealed logging roads which can represent disproportionally large sources of sediment.[55] In addition, the ability of the Puarenga Stream to transport TSS (and hence PP) during its typical range of Q, is likely to be higher due to the high drainage density of the catchment and short distances between headwaters and sampling location (Fig. 2).

Despite generally higher base flow concentrations for nutrient and suspended sediment fractions, estimated yields of TN and TSS were, respectively, either comparable or lower for the Puarenga Stream compared to the Ngongotaha Stream (Table 2). This partly reflects difference in area but also differences in hydrology between the two catchments, as, due to the disproportionate influence of large storm flows on loading (Fig. 8 and Table 1), the occurrence of larger storm flow peaks (reflecting local variation in rainfall between the catchments) compensated for lower loading rates during base flows. Given the unusually high rainfall during the study period, particularly in January of 2011 and 2012, yields calculated in this study are not necessarily representative of longer-term loading for the two catchments. Higher estimated TP yields for the Puarenga Stream catchment reflect the relatively much higher TP concentrations for base flow conditions in this stream and the TP yields are an order of magnitude higher than in another study that estimated TP yield from a pine forested catchment in New Zealand.[56]

Implications for lake water quality and management

Nutrient enrichment experiments have demonstrated both N- and P-limitation of phytoplankton biomass in Lake Rotorua;[57] consequently, excess addition of either nutrient has the potential to promote undesirable phytoplankton growth. The relatively high contribution of dissolved inorganic nitrogen to TN in event loads means rain events have the potential to cause delivery of high loads of labile N to Lake Rotorua over short periods. The implications of this for water quality will depend on ambient physical, chemical and biological conditions; the mechanisms by which storm events mediate phytoplankton resource limitation in lakes are complex, and include enhanced light limitation and increased flushing, in addition to relaxation of nutrient limitation.[58]

By contrast, the extent to which TP transported during hydrological events can be utilised by primary producers downstream is less certain, owing to the high proportion of PP present in TP event loads (Fig. S1b†). The short-term bioavailability of PP in storm flow has been shown to vary from 25–75%

for a hardwater catchment with loamy brown earth soils,[59] although Hatch et al.[60] observed no stimulation of phytoplankton growth following addition of PP associated with particles >0.45 μm sourced from the Lake Tahoe (California, USA) catchment. Due to the lower bioavailability of mineral PP relative to dissolved P, Lewis et al.[61] propose that it may be preferable to use only dissolved P (i.e. PO_4–P) as a basis for assigning loading limits for lakes. Such a policy cannot, however, be endorsed for Lake Rotorua as previous work has highlighted the significance of benthic releases of PO_4 that occur when low oxygen conditions prevail in the hypolimnion (e.g. during summer stratification).[62] Although the chemical composition of PP was not examined in this study, allophanic sediments from the central North Island region of New Zealand can be high in Fe which can form redox-sensitive complexes with PO_4–P.[43,63] Therefore, although stream-borne PP may not be immediately bioavailable in the receiving lake environment, the disproportionally high loading of PP to the lake during high Q that is typically unaccounted during routine monthly monitoring, should be an important consideration for lake managers, given the known status of sediments as the largest source of PO_4–P to the lake over annual periods.[62] Further investigation of P-sorption characteristics (e.g. water-soluble P and equilibrium P concentrations) of TSS and potential sediment sources such as stream banks, channel beds and gully slopes could help to better quantify the potential for PP originated from eroded material to contribute to eutrophication in Lake Rotorua.[64]

The potential for few large events to account for the majority of TSS and TP loading has been observed elsewhere. For example, Salvia-Castellví et al.[14] note that annual TP loads in a rural stream are dominated by TP transported during the rising limb of only a small number of storm events each year. Empirical approaches to load estimation that fail to consider the strong relationship between TP and Q will substantially underestimate TP loads to the lake (Table S3†), while inter-annual variation in the size and frequency of floods means that error may be large if static nutrient export coefficients based on characteristics such as land use are used to estimate nutrient transport in a particular year. Regression or ratio estimation approaches that reflect concentration–Q relationships are therefore preferable, and, in the case of ratio estimators, a stratified approach based on Q_{max} could be used to improve precision. Such techniques are dependent, however, on the availability of event-based samples which are costly and laborious to collect. Dynamic process-based models could potentially resolve issues around accounting for temporal (e.g. due to land use change) and spatial differences in transport processes between sub-catchments and, consequently, aid estimation of pollutant flux where fewer data are available.[65] Such an approach would still though require catchment-specific field data for calibration/validation, and the complex groundwater interactions in the lake catchment also present a challenge to adoption of more mechanistic models.

High temporal inequality in loading shown in this study underlines the importance of best management practices designed to minimise erosion (e.g. ref. 66) for controlling pollutant loads to the lake. Planting of hill slopes, gullies and riparian zones has already been shown to be successful in this regard[67] and manipulating ephemeral surface drainage networks to attenuate storm flow and promote sediment deposition (e.g. by constructing silt traps or detainment bunds) also holds promise for attenuating pollutant loads.[68] The rationale for such sustainable land management practices is further strengthened by the predicted increase in the frequency and magnitude of extreme rainfall events in New Zealand.[69] Increased predicted climatic variability will also likely make it more difficult to characterise trends in lake water quality, i.e. the disproportionate significance of individual high Q events for nutrient loading means that it will be an increasing challenge for lake managers to distinguish changes in lake water quality due to specific management actions from those due to fluctuation in wider hydrological factors.

Acknowledgements

References

1 J. Donohue and G. Molinos, Biol. Rev., 2009, 84, 517–531.
2 R. A. Vollenweider, Scientific fundamentals of the eutrophication of lakes and flowing waters, with particular reference to nitrogen and phosphorus as factors of eutrophication, Organisation for Economic Co-operation and Development, Paris, France, 1968.
3 C. P. Mainstone, R. M. Dils and J. A. Withers, J. Hydrol., 2008, 350, 131–143.
4 D. F. Burger, D. P. Hamilton and C. A. Pilditch, Ecol. Modell., 2008, 211, 411–423.
5 A. L. Collins and D. F. McGonigle, Environ. Sci. Policy, 2008, 11, 97–101.
6 P. Jordan, J. Arnscheidt, H. McGrogan and S. McCormick, Hydrol. Earth Syst. Sci., 2005, 9, 685–691.
7 M. Chiwa, J. Ide, R. Maruno, N. Higashi and K. Otsuki, Hydrol. Processes, 2010, 24, 631–640.
8 P. J. Johnes, J. Hydrol., 2007, 332, 241–258.
9 H. S. Lim, Hydrobiologia, 2003, 494, 57–63.
10 K. Guan, S. E. Thompson, C. J. Harman, N. B. Basu, P. S. C. Rao, M. Sivapalan, A. I. Packman and P. K. Kalita, Water Resour. Res., 2011, 47, W00J02.
11 J. W. Kirchner, X. H. Feng and C. Neal, Nature, 2000, 403, 524–527.
12 D. B. Lewis and N. B. Grimm, Ecol. Appl., 2007, 17, 2347–2364.

13 T. Kato, H. Kuroda and H. Nakasone, *J. Hydrol.*, 2009, **368**, 79–87.

14 M. Salvia-Castellví, J. P. Iffly, P. V. Borght and L. Hoffmann, *Sci. Total Environ.*, 2005, **344**, 51–65.

15 Z. Zhang, F. Tao, P. Shi, W. Xu, Y. Sun, T. Fukushima and Y. Onda, *Hydrol. Processes*, 2010, **24**, 2960–2970.

16 J. C. Rozemeijer, Y. Van der Velde, F. C. Van Geer, G. H. De Rooij, P. Torfs and H. P. Broers, *Environ. Sci. Technol.*, 2010, **44**, 6305–6312.

17 M. J. Bowes, W. A. House, R. A. Hodgkinson and D. V. Leach, *Water Res.*, 2005, **39**, 751–762.

18 W. A. House and M. S. Warwick, *Water Res.*, 1998, **32**, 2279–2290.

19 D. Burns, *Hydrol. Processes*, 2005, **19**, 1325–1327.

20 A. B. Atkinson, *J. Econ. Theor.*, 1970, **2**, 244–263.

21 J. W. Jawitz and J. Mitchell, *Water Resour. Res.*, 2011, **47**, W00J14.

22 J. P. Siwek, M. Zelazny and W. Chelmicki, *Water, Air, Soil Pollut.*, 2011, **214**, 547–563.

23 K. A. Lohse, P. D. Brooks, J. C. McIntosh, T. Meixner and T. E. Huxman, *Annual Review of Environment and Resources*, Annual Reviews, Palo Alto, 2009, pp. 65–96.

24 R. A. Letcher, A. J. Jakeman, M. Calfas, S. Linforth, B. Baginska and I. Lawrence, *Environ. Modell. Software*, 2002, **17**, 77–85.

25 B. Boström, G. Persson and B. Broberg, *Hydrobiologia*, 1988, **170**, 133–155.

26 D. A. Bronk, J. H. See, P. Bradley and L. Killberg, *Biogeosciences*, 2007, **4**, 283–296.

27 U. Morgenstern, R. Reeves, C. Daughney, S. Cameron and D. Gordon, *Groundwater Age and Chemistry, and Future Nutrient Loads for Selected Rotorua Lakes Catchments*, Institute of Geological and Nuclear Sciences, Lower Hutt, New Zealand, 2005, p. 82.

28 P. J. F. Newsome, R. H. Wilde and E. J. Willoughby, *Land and Resource Infomation Sytem Spatial Data Layers Volume 1: 'Label Format'*, Landcare Research, Palmerston North, New Zealand, 2000.

29 Parliamentary Commissioner for the Environment, *Restoring the Rotorua Lakes: The Ultimate Endurance Challenge*, Wellington, New Zealand, 2006.

30 J. C. Rutherford, *N. Z. J. Mar. Freshwater Res.*, 1984, **18**, 355–365.

31 R. A. Hoare, *J. Hydrol.*, 1980, **19**, 49–59.

32 J. C. Rutherford and G. Timpany, *Storm Nutrient Loads in Rotorua Streams*, National Institute for Water and Atmospheric Science, 2008, p. 71.

33 M. Tomer, C. Smith, A. Thorn, G. Gielen, T. Chaleston and L. Barton, Evaluation of Treatment Performance and Processes after Six Years of Wastewater Application at Whakarewarewa Forest, New Zealand, in *The forest alternative: Principles and practice of residuals use*, ed. C. Henry, R. Harrison and P. Bastian. University of Washington, Seattle, 2000.

34 American Public Health Association, *Standard Methods for the Examination of Water and Wastewater*, Washington, DC, 20th edn, 1998.

35 S. D. Preston, V. J. Bierman and S. E. Silliman, *Water Resour. Res.*, 1989, **25**, 1379–1389.

36 R. I. Ferguson, *Water Resour. Res.*, 1986, **22**, 74–76.

37 National Institute of Water and Atmospheric Research, *Annual New Zealand Climate Statistics 2011–2012*, http://www.niwa.co.nz, accessed 06 December 2012.

38 National Institute of Water and Atmospheric Research, *Environmental Data Explorer New Zealand*, http://edenz.niwa.co.nz/, accessed 04 December 2012.

39 M. J. Vanni, W. H. Renwick, J. L. Headworth, J. D. Auch and M. H. Schaus, *Biogeochemistry*, 2001, **54**, 85–114.

40 Q. Zhu, J. P. Schmidt, A. R. Buda, R. B. Bryant and G. J. Folmar, *J. Hydrol.*, 2011, **405**, 307–315.

41 C. Oeurng, S. Sauvage and J. M. Sanchez-Perez, *Sci. Total Environ.*, 2010, **409**, 140–149.

42 P. Haygarth, B. L. Turner, A. Fraser, S. Jarvis, T. Harrod, D. Nash, D. Halliwell, T. Page and K. Beven, *Hydrol. Earth Syst. Sci.*, 2004, **8**, 88–97.

43 R. L. Parfitt, *Aust. J. Soil Res.*, 1990, **28**, 343–360.

44 L. M. Mayer and S. P. Gloss, *Limnol. Oceanogr.*, 1980, **25**, 12–22.

45 J. J. Drewry, L. T. H. Newham and B. F. W. Croke, *J. Environ. Manage.*, 2009, **90**, 879–887.

46 M. I. Stutter, S. J. Langan and R. J. Cooper, *J. Hydrol.*, 2008, **350**, 203–214.

47 R. W. McDowell, B. J. F. Biggs, A. N. Sharpley and L. Nguyen, *Chem. Ecol.*, 2004, **20**, 1–40.

48 S. T. Larned, M. R. Scarsbrook, T. H. Snelder, N. J. Norton and B. J. F. Biggs, *N. Z. J. Mar. Freshwater Res.*, 2004, **38**, 347–366.

49 J. D. Allan, *Annu. Rev. Ecol. Evol. Systemat.*, 2004, **35**, 257–284.

50 J. C. Rutherford, C. Palliser and S. Wadhwa, *Prediction of Nitrogen Loads to Lake Rotorua Using the ROTAN Model*, National Institutefor Water and Atmospheric Research, Hamilton, 2011, p. 183.

51 R. A. Hoare, *N. Z. J. Mar. Freshwater Res.*, 1982, **16**, 339–349.

52 G. N. Magesan, C. D. A. McLay and V. V. Lal, *Agric., Ecosyst. Environ.*, 1998, **70**, 181–187.

53 J. M. Quinn and M. J. Stroud, *N. Z. J. Mar. Freshwater Res.*, 2002, **36**, 409–429.

54 J. de Vente and J. Poesen, *Earth-Sci. Rev.*, 2005, **71**, 95–125.

55 P. N. J. Lane and G. J. Sheridan, *Hydrol. Processes*, 2002, **16**, 2599–2612.

56 A. B. Cooper and C. E. Thomsen, *N. Z. J. Mar. Freshwater Res.*, 1988, **22**, 279–291.

57 D. F. Burger, D. P. Hamilton, J. A. Hall and E. F. Ryan, *Fundam. Appl. Limnol.*, 2007, **169**, 57–68.

58 M. J. Vanni, J. S. Andrews, W. H. Renwick, M. J. Gonzalez and S. J. Noble, *Arch. Hydrobiol.*, 2006, **167**, 421–445.

59 N. Pacini and R. Gachter, *Biogeochemistry*, 2009, **47**, 87–109.

60 L. K. Hatch, J. E. Reuter and C. R. Goldman, *Can. J. Fish. Aquat. Sci.*, 1999, **56**, 2331–2339.

61 W. M. Lewis, W. A. Wurtsbaugh and H. W. Paerl, *Environ. Sci. Technol.*, 2011, **45**, 10300–10305.

62 D. F. Burger, D. P. Hamilton, C. A. Pilditch and M. M. Gibbs, *Hydrobiologia*, 2007, **584**, 13–25.

63 D. J. Evans, P. J. Johnes and D. S. Lawrence, *Sci. Total Environ.*, 2004, **329**, 165–182.

64 R. Pothig, H. Behrendt, D. Opitz and G. Furrer, *Environ. Sci. Pollut. Res.*, 2010, **17**, 497–504.

65 A. J. Wade, B. M. Jackson and D. Butterfield, *Sci. Total Environ.*, 2008, **400**, 52–74.

66 R. W. McDowell and D. Nash, *J. Environ. Qual.*, 2012, **41**, 680–693.

67 R. B. Williamson, C. M. Smith and A. B. Cooper, *J. Water Resour. Plann. Manag.*, 1996, **122**, 24–32.

68 J. M. Abell, D. P. Hamilton and J. Paterson, *Australasian Journal of Environmental Management*, 2011, **18**, 139–154.

69 Intergovernmental Panel on Climate Change, Fourth Assessment Report: Climate Change. 2007 Working Group II Report, *Impacts, Adaptation and Vulnerability*, Cambridge University Press, Cambridge, United Kingdom, 2007.